



Title	Nucleophilic reactions of bromocyclopentane in the structure-h methane + bromocyclopentane mixed hydrate system at high pressures
Author(s)	Matsumoto, Yuuki; Katsuta, Yoshito; Kamo, Fumitaka et al.
Citation	Journal of Physical Chemistry B. 2014, 118(47), p. 13404-13408
Version Type	AM
URL	https://hdl.handle.net/11094/100987
rights	© 2014 American Chemical Society.
Note	

The University of Osaka Institutional Knowledge Archive : OUKA

<https://ir.library.osaka-u.ac.jp/>

The University of Osaka

Nucleophilic Reactions of Bromocyclopentane in the Structure-H Methane+Bromocyclopentane Mixed Hydrate System at High Pressures

Yuuki Matsumoto¹, Yoshito Katsuta¹, Fumitaka Kamo¹, Tatsuya Bando¹, Takashi Makino², Takeshi Sugahara^{1,}, Kazunari Ohgaki¹*

¹ Division of Chemical Engineering, Department of Materials Engineering Science, Graduate School of Engineering Science, Osaka University, 1-3 Machikaneyama, Toyonaka, Osaka 560-8531, Japan

² National Institute of Advanced Industrial Science and Technology, 4-2-1 Nigatake, Miyagino, Sendai, Miyagi 983-8551, Japan

ABSTRACT. Thermodynamic stability boundary in the structure-H methane+bromocyclopentane mixed hydrate system was measured at pressures from 20 MPa to 100 MPa. The thermodynamic stability boundary of the methane+bromocyclopentane mixed hydrate exhibits anomalous behavior under conditions at high pressures and high temperatures. This phenomenon is due to the elimination and substitution reactions of bromocyclopentane to cyclopentene and cyclopentanol, respectively. The nucleophilic reactions of bromocyclopentane are mainly advanced in the liquid bromocyclopentane-rich phases, while it is restrained when bromocyclopentane is enclathrated in hydrate cage.

KEYWORDS. Clathrate hydrate; Elimination; Substitution; Raman spectroscopy; Structural phase transition

INTRODUCTION

Clathrate hydrate is a solid crystalline, which has an ice-like appearance. Hydrate is necessarily composed of host species and guest species, where the former is water and the latter is generally small molecules such as light hydrocarbons and noble gases. Several water molecules construct cage structures and a cage can normally enclathrate one guest molecule. There are several kinds of hydrate cages.¹ For instance, 5^{12} -cage is a dodecahedron, which is constructed from twelve pentagons. In the same manner, $4^35^66^3$ -cage, $5^{12}6^2$ -cage, $5^{12}6^4$ -cage, and $5^{12}6^8$ -cage are dodecahedron, tetrakaidekahedron, hexakaidecahedron, and icosahedron, respectively. Some of them are combined to form specific hydrate structures. The unit cell of the structure-I (s-I) hydrate consists of two 5^{12} -cages and six $5^{12}6^2$ -cages. In the same manner, that of the structure-II (s-II) hydrate is formed with 16 5^{12} -cages and eight $5^{12}6^4$ -cages. The unit cell of structure-H (s-H) hydrate is composed of three 5^{12} -cages, two $4^35^66^3$ -cages, and one $5^{12}6^8$ -cage.² Simple hydrate is formed with a binary mixture of host species and single guest species. On the other hand, mixed hydrate is formed with more than ternary mixture that is host species and two or more kinds of guest species. Crystal structures and thermodynamic stabilities of hydrates depend on the thermodynamic conditions (pressure, temperature, composition, etc.) and the properties of guest species (size, shape, molar volume, molar weight, solubility, polarity, etc.).^{1,3} A lot of guest species have been reported until now.¹ As special, the guest species normally occupying $5^{12}6^8$ -cage cannot form s-H hydrate solely except at extremely high

pressures.^{4,5} When the small guest species such as methane (CH₄) and xenon are added, large guest species (LGS) occupy the 5¹²6⁸-cages of s-H hydrates with the support of small guest species occupying the 5¹²- and 4³5⁶6³-cages.² This is why the small guest species is called “help gas”. In an s-H mixed hydrate, small and large guest species occupy small (5¹²-cage and 4³5⁶6³-cage) and large (5¹²6⁸-cage) cages, respectively, that is, the occupancy form of the s-H mixed hydrate is compartmental.

In the present study, CH₄ and bromocyclopentane (*c*-C₅H₉Br) were adopted as help gas and LGS forming s-H hydrates, respectively. Recently, it has been reported that *c*-C₅H₉Br is an s-H hydrate former.⁶⁻⁸ *c*-C₅H₉Br is relatively small among LGSs forming s-H mixed hydrates. It is very interesting to investigate the high-pressure stability of s-H hydrates having large space around LGS in the 5¹²6⁸-cage, because it has been reported that the large space around a guest molecule results in the instability of the original hydrate structure at high pressures.⁹⁻¹¹ The hydrate stability boundary and the cage occupancy of guest species in the CH₄+*c*-C₅H₉Br mixed hydrate system were clarified by means of phase equilibrium measurement and Raman spectroscopy, respectively.

EXPERIMENTAL

The materials used in the present study are summarized in Table 1. All of them were used without further purification.

Table 1. Information on the Chemicals Used in the Present Study

material name	source	mole fraction purity
methane (CH ₄)	Liquid Gas Co., Ltd.	> 0.9999
bromocyclopentane (<i>c</i> -C ₅ H ₉ Br)	Merck Ltd.	> 0.99
cyclopentene (<i>c</i> -C ₅ H ₈)	Tokyo Chemical Industries Co., Ltd.	> 0.95
cyclopentanol (<i>c</i> -C ₅ H ₉ OH)	Merck Ltd.	> 0.99
water	Wako Pure Chemicals Ind., Ltd.	> 0.9999

The experimental apparatus used in the present study is almost the same as ones used in the previous work (except for using the different type of high-pressure optical cell).¹² In the present study, the high-pressure optical cell with sapphire windows (inner volume: 0.2 cm³, maximum working pressure: 400 MPa) was used for the phase equilibrium measurement and *in-situ* Raman spectroscopy. Equilibrium pressure was measured by three kinds of pressure gauges according to the working pressures. Below 10 MPa, the equilibrium pressure was measured with a pressure gauge (VALCOM VPRT, maximum uncertainty: 0.02 MPa). At pressures of 10–100 MPa, the pressure gauge (VALCOM VPRT) was used with a maximum uncertainty of 0.2 MPa. Above 100 MPa, a pressure transducer (NMB STD-5000K) and digital peak holder (NMB CSD-819) were used with the estimated maximum uncertainty of 2 MPa. Programming thermocontroller (EYELA NCB-3100) adjusted the cell temperature. Equilibrium temperature was measured with a thermistor probe (TAKARA D-641). The maximum uncertainty of equilibrium temperature

was 0.02 K. A laser Raman microprobe spectrometer with a multichannel charge-coupled device (CCD) detector (JOBIN-YVON Ramanor T64000) and an argon ion laser beam (514.5 nm, 100 mW) condensed to 2 μm in spot diameter were used to analyze hydrate single crystals. The CCD detector was maintained at 140 K by liquid nitrogen for heat-noise reduction. The spectral resolution was approximately 0.7 cm^{-1} . The Raman shift ($\Delta\nu$) was calibrated with the neon emission lines in the air.

For the phase equilibrium measurement, a desired amount of *c*-C₅H₉Br was introduced into the high-pressure optical cell. After removal of the dissolved air, CH₄ was introduced into the cell up to a desired pressure. After that, the contents were pressurized with distilled water with use of a high-pressure pump. The contents were cooled and agitated to generate mixed hydrates. After the hydrate formation, the temperature was gradually increased and decreased respectively to establish a four-phase coexistence condition. When the pressure became constant and the four-phase coexistence was confirmed visually, we determined that the system reached a four-phase equilibrium and recorded a pressure and a temperature as an equilibrium datum set.

For the Raman spectroscopy, the hydrate single crystal was prepared in order to obtain a clear and reproducible Raman spectrum. After the mixed-gas hydrates were generated in a high-pressure optical cell, the temperature was gradually increased and decreased to prepare hydrate single crystals. Then the single crystals were annealed to avoid metastability, and the temperature was kept constant for more than one day to establish the phase equilibrium conditions. The hydrate single crystal and the *c*-C₅H₉Br-rich liquid phase were analyzed by use of Raman spectrometer with multichannel CCD detector. The argon ion laser beam was irradiated from the object lens to each phase through the upper sapphire window.

In the phase equilibrium and Raman spectroscopic measurements, the hydrate crystals never failed to be decomposed before moving toward the following equilibrium point. The phase behavior was observed straightforwardly with a CCD camera through the sapphire window.

RESULTS AND DISCUSSION

The phase equilibrium relation in the $\text{CH}_4+c\text{-C}_5\text{H}_9\text{Br}$ mixed hydrate system is shown in Figure 1. In the whole experimental pressure and temperature range of the present study, the four-phase equilibrium curve of (hydrate, aqueous, *c*- $\text{C}_5\text{H}_9\text{Br}$ -rich liquid, and gas phases) in the $\text{CH}_4+c\text{-C}_5\text{H}_9\text{Br}$ mixed hydrate system is laid at a pressure lower (a temperature higher) than the three-phase equilibrium (hydrate, aqueous, and fluid phases) curve in the simple CH_4 hydrate system. At low pressures and low temperatures, the equilibrium data of the $\text{CH}_4+c\text{-C}_5\text{H}_9\text{Br}$ mixed hydrate system have been reported.^{6,8} The equilibrium data plotted by solid keys below 80 MPa would be smoothly connected with the reported data^{6,8} in the low-pressure region. Raman spectra derived from the CH_4 and *c*- $\text{C}_5\text{H}_9\text{Br}$ molecules in the hydrate phase are shown in Figure 2, which is accompanied with the Raman spectra corresponding to the intermolecular vibration between water molecules (lattice mode). The Raman peak of the intramolecular C–Br stretching vibration mode of *c*- $\text{C}_5\text{H}_9\text{Br}$ was detected around 520 cm^{-1} at (2.90 MPa and 278.20 K) and (58.6 MPa and 300.35 K). The peak of the C–H symmetric stretching vibration mode of CH_4 was also detected at 2913 cm^{-1} , which agrees well with that in the s-H hydrates.¹⁴⁻¹⁶

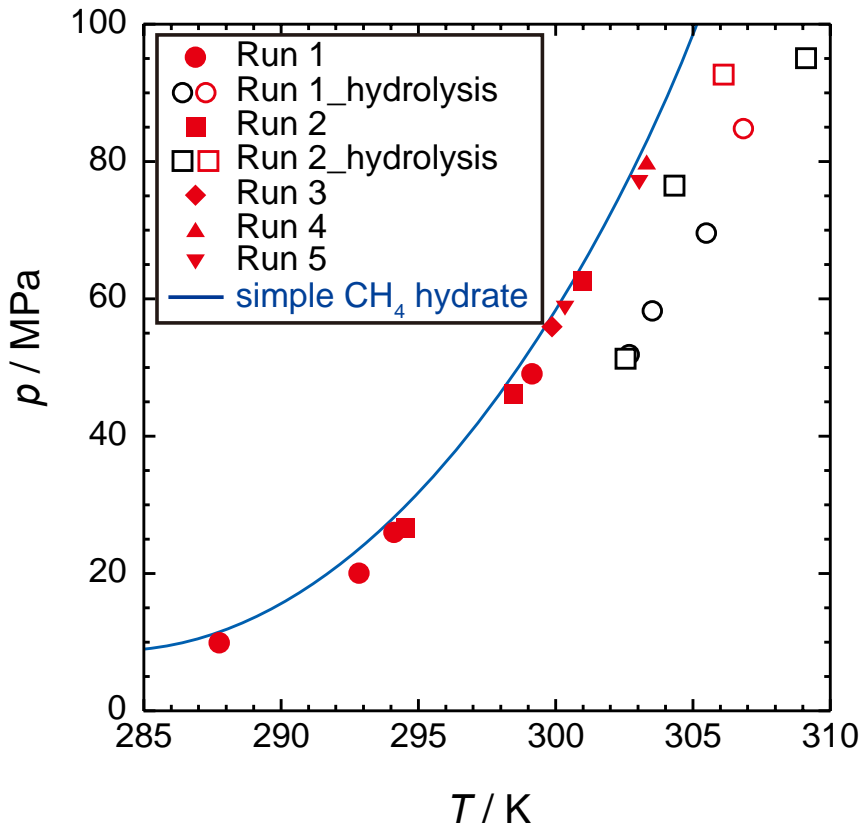


Figure 1. Four-phase equilibrium relation of (hydrate, aqueous, *c*-C₅H₉Br-rich liquid, and gas phases) in the s-H CH₄+*c*-C₅H₉Br mixed hydrate system (Closed keys). Open red keys, located at (84.8 MPa, 306.84 K in run 1) and (92.7 MPa, 306.12 K in run 2), represent the points where the considerable nucleophilic reactions of *c*-C₅H₉Br was recognized in each run. Open black keys represent the phase equilibrium data measured subsequently under different conditions after the recognition of the considerable nucleophilic reactions of *c*-C₅H₉Br. Solid blue curve is the three-phase equilibrium curve of (hydrate, aqueous, and gas phases) in the simple CH₄ hydrate system^{4,13}.

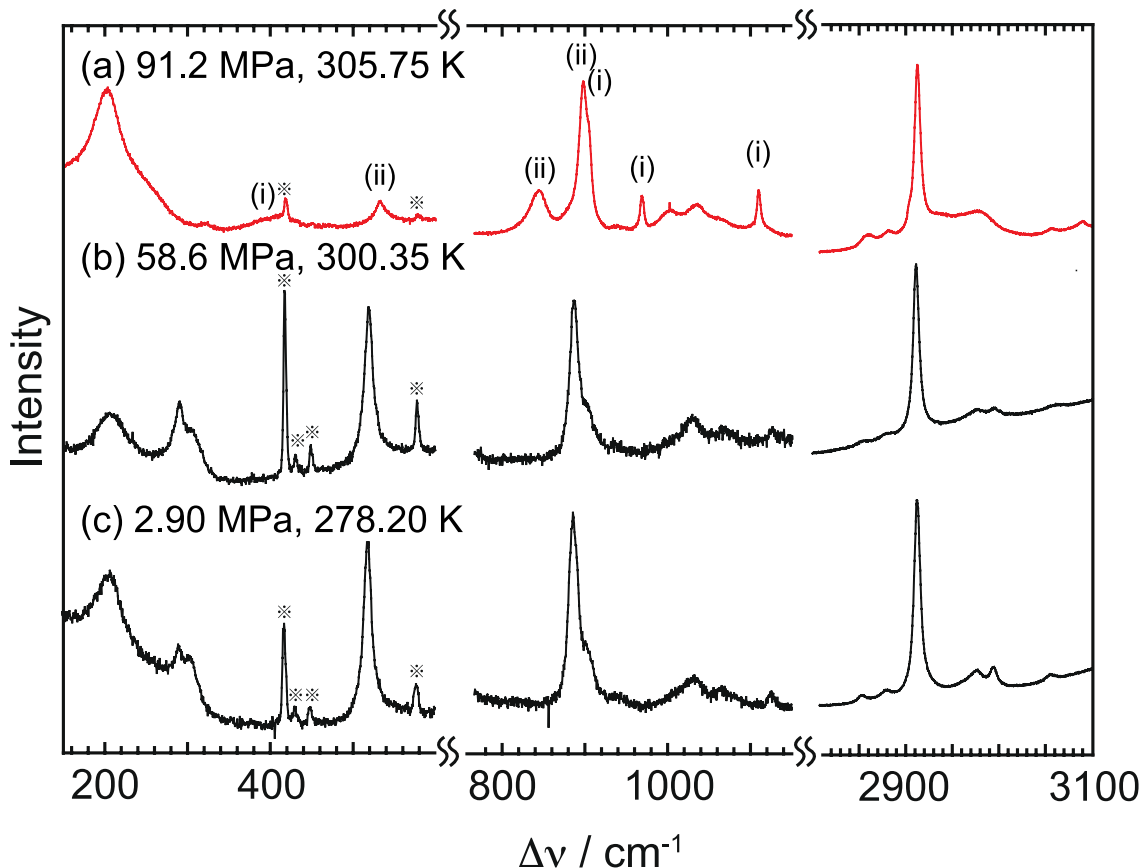


Figure 2. Raman spectra obtained from hydrate phase in the $\text{CH}_4 + c\text{-C}_5\text{H}_9\text{Br}$ mixed hydrate system. The peaks marked by the symbols (i) and (ii) are derived from the $c\text{-C}_5\text{H}_8$ and $c\text{-C}_5\text{H}_9\text{OH}$, respectively (except for the peaks overlapped with those derived from $c\text{-C}_5\text{H}_9\text{Br}$). Reference marks represent the peaks derived from the sapphire window of the cell.

With further increasing pressure beyond 80 MPa, the Raman spectrum obtained at (91.2 MPa and 305.75 K) shown in Figure 2a was drastically changed. In addition, at pressures above 80 MPa, the equilibrium points measured in the present study were scattered and dependent on the experimental runs (the amount of the introduced $c\text{-C}_5\text{H}_9\text{Br}$ was slightly different in each run). According to Gibbs phase rule, as long as the system components are stationary, the four-phase equilibrium point in a ternary system should be drawn as a curve. This phenomenon may be due

to a pressure-induced structural phase transition in the hydrate phase or a chemical reaction such as the hydrolysis of *c*-C₅H₉Br. If it was caused by the pressure-induced structural phase transition of hydrate phase, the equilibrium points are not scattered but should lie on two curves of metastable and equilibrium conditions. Therefore, a possible cause is a chemical reaction, not just the structural phase transition. After the system sufficiently experienced at a pressure above 80 MPa (plotted by open red keys in Figure 1), the phase equilibrium relations subsequently measured below 80 MPa (plotted by open black keys) are different from the original ones. The result also supports the occurrence of a chemical reaction. Unfortunately, it is difficult to take the contents from the high-pressure optical cell because of its tiny inner volume. In order to determine the reaction products, Raman spectrum detected in the *c*-C₅H₉Br-rich liquid phase of the CH₄+*c*-C₅H₉Br+water ternary system was compared with those of the *c*-C₅H₉Br+water (without CH₄ before stirring) and cyclopentene(*c*-C₅H₈)+water binary systems (measured at similar pressures without gas by means of the volume-changeable high-pressure cell¹²) as shown in Figure 3. Comparing the spectra between Figure 3a and 3b, the additional peaks unlike *c*-C₅H₉Br were detected around 960, 1100, 1300, and 1620 cm⁻¹ in the spectrum obtained from CH₄+*c*-C₅H₉Br+water system. These peaks agree with some of the peaks derived from *c*-C₅H₈ (Figure 3c), although the positions of the emerging peaks in Figure 3b are approximately 1 cm⁻¹ higher than those in Figure 3c. The peak shifts would be caused by the different circumstances surrounding a *c*-C₅H₈ molecule, that is, in the *c*-C₅H₉Br-rich liquid phase (Figure 3b) and the *c*-C₅H₈-rich liquid phase (Figure 3c). With further hydrolyzing *c*-C₅H₉Br, the peaks derived from cyclopentanol (*c*-C₅H₉OH) also appear. That is, *c*-C₅H₉Br is transformed to *c*-C₅H₈ and *c*-C₅H₉OH by the elimination and substitution reactions. As shown in Figure 4, the silver nitrate reaction reveals the existence of Br anion in the recovered aqueous phase. In this system, water

exists as the solvent, which works as a weak nucleophile, and it causes elimination and substitution reactions. The nucleophilic reactions of *c*-C₅H₉Br slightly occur even at low pressures according to the silver nitrate reaction but the reactivity is not too high. Therefore, the formed amounts of *c*-C₅H₈ and *c*-C₅H₉OH are negligible and the phase equilibrium curve seems to be independent. At high pressures and high temperatures, these nucleophilic reactions become remarkable and considerable. The reaction products (*c*-C₅H₈ and *c*-C₅H₉OH) are also enclathrated, because it is reported that the *c*-C₅H₈ molecule is enclathrated in the 5¹²6⁴-cage of s-II hydrate.^{17,18} Moreover, the four-phase equilibrium curves in the CH₄+*c*-C₅H₈ and CH₄+*c*-C₅H₉OH mixed hydrate systems are laid at a pressure lower (a temperature higher) than that in the CH₄+*c*-C₅H₉Br system^{6,8} as shown in Figure 5 (Supporting Information, Table S1). The drastic change of the Raman spectrum in Figure 2a indicates that *c*-C₅H₈ and *c*-C₅H₉OH as well as a quite small amount of *c*-C₅H₉Br competitively occupy the 5¹²6⁴-cages of the s-II hydrate in this system. The molecular sizes of *c*-C₅H₈ and *c*-C₅H₉OH are smaller than that of *c*-C₅H₉Br and they would be too small for the 5¹²6⁸-cage stabilization.

When hydrate-free CH₄+*c*-C₅H₉Br+water system was pressurized up to 100 MPa and kept at 306 K for a couple of days, *c*-C₅H₉Br was well hydrolyzed. On the other hand, the s-H CH₄+*c*-C₅H₉Br mixed hydrates prepared at 50 MPa was pressurized up to 100 MPa without the destruction of hydrate. After 4 days at 304 K, the nucleophilic reactions of *c*-C₅H₉Br enclathrated in hydrate cage were not observed. That is, the nucleophilic reactions of *c*-C₅H₉Br are restrained while *c*-C₅H₉Br is enclathrated in hydrate cage. The nucleophilic reactivity of the water molecules incorporated in the hydrate framework would be lower than that in aqueous phase. The novel reaction system, where the decomposition of the hydrate framework is treated as a trigger of a subsequent reaction, might be developed. It has been reported that the hydrate

cage, as long as the hydrate does not decomposed, has the ability for the preservation of the reactive species, such as methyl radicals,²⁰⁻²² hydrogen atom,²³ and ozone²⁴.

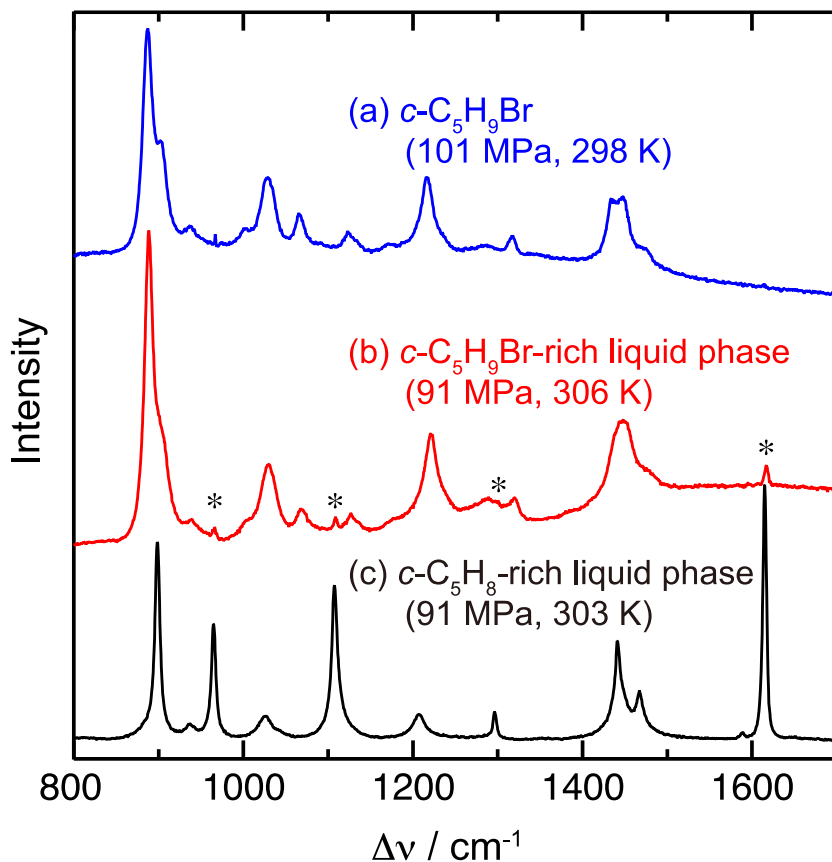


Figure 3. Raman spectra of cyclopentane-derivatives in (a) $c\text{-C}_5\text{H}_9\text{Br}$ liquid phase (before stirring the liquid-liquid interface between $c\text{-C}_5\text{H}_9\text{Br}$ and water) (without CH_4); (b) $c\text{-C}_5\text{H}_9\text{Br}$ -rich liquid phase coexisted with the aqueous and hydrate phases; and (c) $c\text{-C}_5\text{H}_8$ -rich liquid phase coexisted with the aqueous phase. The asterisks stand for the emerging peaks resulting from the nucleophilic reactions. The positions of the emerging peaks agree with that derived from $c\text{-C}_5\text{H}_8$.

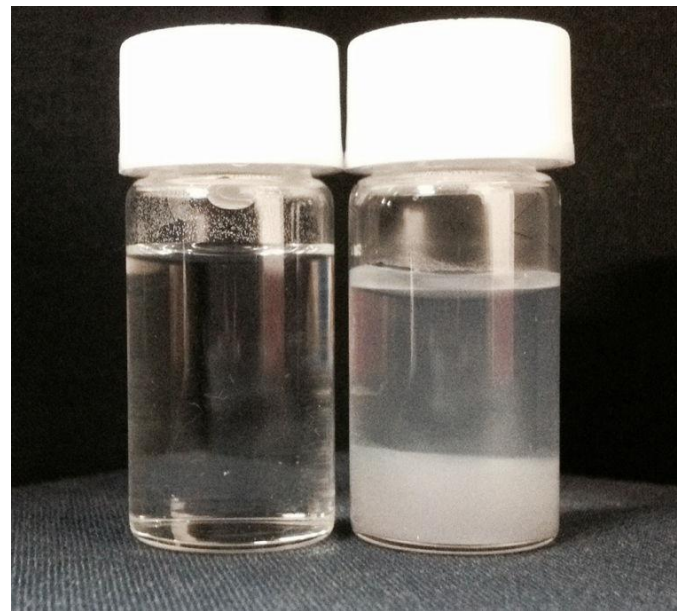


Figure 4. Silver nitrate reaction in the diluted aqueous phase coexisted with *c*-C₅H₉Br-rich liquid phase. The left and right bottles are without and with silver nitrate, respectively.

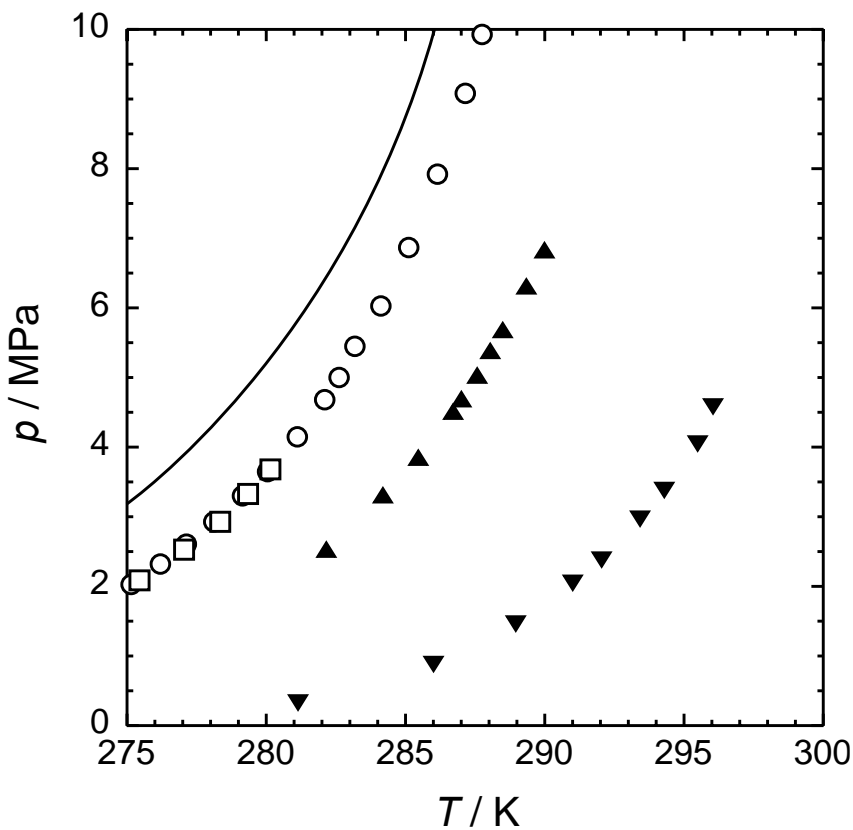


Figure 5. Four-phase equilibrium relations of (hydrate, aqueous, cyclopentane-derivative rich liquid, and gas phases) in the $\text{CH}_4+c\text{-C}_5\text{H}_9\text{Br}$ (open squares, ref 6; open circles, ref 8), $\text{CH}_4+c\text{-C}_5\text{H}_8$ (closed inverted triangles, measured in the present study), and $\text{CH}_4+c\text{-C}_5\text{H}_9\text{OH}$ (closed triangles, measured in the present study) mixed hydrate systems. Solid curve is the three-phase equilibrium curve of (hydrate, aqueous, and gas phases) in the simple CH_4 hydrate system.¹⁹

CONCLUSION

The thermodynamic stability boundary of the $\text{CH}_4+c\text{-C}_5\text{H}_9\text{Br}$ mixed hydrate was investigated. At pressures higher than around 80 MPa, anomalous behavior in the stability boundary and the Raman spectra were observed, which is caused by the elimination and substitution reactions of *c*-

C_5H_9Br in the *c*- C_5H_9Br -rich liquid phase. The hydrate cage prevents the *c*- C_5H_9Br molecule from the nucleophilic reactions even at pressures above 80 MPa, while *c*- C_5H_9Br in liquid phase is hydrolyzed into *c*- C_5H_8 or *c*- C_5H_9OH .

AUTHOR INFORMATION

Corresponding Author

* Tel.&Fax.: +81-6-6850-6293. E-mail: sugahara@cheng.es.osaka-u.ac.jp

Funding Sources

This work was partially supported by KAKENHI, Grant-in-Aid for JSPS Fellows (25·1430) (YM), Grant-in-Aid for Young Research (B) (22710081) (TM) and the Kansai Research Foundation for technology promotion (TM).

Notes

The authors declare no competing financial interest.

Supporting Information

Four-phase equilibrium relations in the CH_4 +cyclopentene and CH_4 +cyclopentanol mixed hydrate systems are summarized in Table S1. This material is available free of charge via the Internet at <http://pubs.acs.org>.

ACKNOWLEDGMENT

We also acknowledge the scientific supports from the “Gas-Hydrate Analyzing System (GHAS)” of the Division of Chemical Engineering, Graduate School of Engineering Science, Osaka

University. We thank Dr. H. Sato (Osaka University) for the valuable discussion and suggestions.

REFERENCES

- (1) Sloan, E.D.; Koh, C.A. *Clathrate Hydrates of Natural Gases*, 3rd ed.; Taylor & Francis-CRC Press: Boca Raton, FL, 2008.
- (2) Ripmeester, J. A.; Tse, J. S.; Ratcliffe, C. I.; Powell, B. M. A New Clathrate Hydrate Structure. *Nature* **1987**, *325*, 135–136.
- (3) Tezuka, K.; Taguchi, T.; Alavi, S.; Sum, A.K.; Ohmura, R. Thermodynamic Stability of Structure H Hydrates Based on the Molecular Properties of Large Guest Molecules. *Energies* **2012**, *5*, 459–465.
- (4) Dyadin, Y. A.; Aladko, E. Y.; Larionov, E. G. Decomposition of Methane Hydrates up to 15 kbar. *Mendeleev Commun.* **1997**, *7*, 34–35.
- (5) Kumazaki, T.; Kito, Y.; Sasaki, S.; Kume, T.; Shimizu, H. Single-Crystal Growth of the High-Pressure Phase II of Methane Hydrate and Its Raman Scattering Study. *Chem. Phys. Lett.* **2004**, *388*, 18–22.
- (6) Jin, Y.; Kida, M.; Nagao, J. Structure H (sH) Clathrate Hydrate with New Large Molecule Guest Substances. *J. Phys. Chem. C* **2013**, *117*, 23469–23475.
- (7) Jin, Y.; Kida, M.; Nagao, J. Crystal Phase Boundaries of Structure - H (sH) Clathrate Hydrates with Rare Gas (Krypton and Xenon) and Bromide Large Molecule Guest Substances. *J. Chem. Eng. Data* **2014**, *59*, 1704–1709.

(8) Matsumoto, Y.; Matsukawa, H.; Kamo, F.; Jeon, Y. B.; Katsuta, Y.; Bando, T.; Makino, T.; Sugahara, T.; Ohgaki, K. Thermodynamic Stability Boundaries and Structures of Methane+Monohalogenated Cyclopentane Mixed Hydrates. *J. Chem. Eng. Data* **2014**, *59*, 2294–2297.

(9) Sugahara, K.; Yoshida, M.; Sugahara, T.; Ohgaki, K. Thermodynamic and Raman Spectroscopic Studies on Pressure-Induced Structural Transition of SF₆ Hydrate. *J. Chem. Eng. Data* **2006**, *51*, 301–304.

(10) Dyadin, Y.A.; Larionov, E.G.; Aladko, E.Y.; Zhurko, F.V. Clathrate Formation in Propane-Water and Methane-Propane-Water Systems under Pressures of up to 15 kbar. *Doklady Phys. Chem.* **2001**, *376*, 23–26.

(11) Katsuta, Y.; Suzuki, S.; Matsumoto, Y.; Hashimoto, S.; Sugahara, T.; Ohgaki, K. Phase Equilibrium Relations and Structural Transition in the 1,1,1,2-Tetrafluoroethane Hydrate System. *J. Chem. Eng. Data* **2013**, *58*, 1378–1381.

(12) Nakano, S.; Moritoki, M.; Ohgaki, K. High-Pressure Phase Equilibrium and Raman Microprobe Spectroscopic Studies on the CO₂ Hydrate System. *J. Chem. Eng. Data* **1998**, *43*, 807–810.

(13) Nakano, S.; Moritoki, M.; Ohgaki, K. High-Pressure Phase Equilibrium and Raman Microprobe Spectroscopic Studies on the Methane Hydrate System. *J. Chem. Eng. Data* **1999**, *44*, 254–257.

(14) Makino, T.; Mori, M.; Mutou, Y.; Sugahara, T.; Ohgaki, K. Four-Phase Equilibrium Relations of Methane + Methylcyclohexanol Stereoisomer + Water Systems Containing Gas Hydrate. *J. Chem. Eng. Data* **2009**, *54*, 996–999.

(15) Matsumoto, Y.; Miyauchi, H.; Makino, T.; Sugahara, T.; Ohgaki, K. Structural Phase Transitions of Methane+Ethane Mixed-Gas Hydrate Induced by 1,1-Dimethylcyclohexane. *Chem. Eng. Sci.* **2011**, *66*, 2672–2676.

(16) Suzuki, S.; Matsumoto, Y.; Katsuta, Y.; Hashimoto. S.; Sugahara, T.; Ohgaki, K. Structure-H Methane + 1,1,2,2,3,3,4-Heptafluorocyclopentane Mixed Hydrate at Pressures up to 373 MPa. *J. Phys. Chem. A* **2013**, *117*, 4338–4341.

(17) Takeya, S.; Ohmura, R. Phase Equilibrium for Structure II Hydrates Formed with Krypton Co-existing with Cyclopentane, Cyclopentene, or Tetrahydropyran. *J. Chem. Eng. Data* **2006**, *51*, 1880–1883.

(18) Takeya, S.; Yasuda, K.; Ohmura, R. Phase Equilibrium for Structure II Hydrates Formed with Methylfluoride Coexisting with Cyclopentane, Fluorocyclopentane, Cyclopentene, or Tetrahydropyran. *J. Chem. Eng. Data* **2008**, *53*, 531–534.

(19) Nakamura, T.; Makino, T.; Sugahara, T.; Ohgaki, K. Stability Boundaries of Gas Hydrates Helped by Methane – Structure-H Hydrates of Methylcyclohexane and *cis*-1,2-Dimethylcyclohexane. *Chem. Eng. Sci.* **2003**, *58*, 269–273.

(20) Takeya, K.; Tani, A.; Yada, T.; Ikeya, M.; Ohgaki, K. Electron Spin Resonance Study on γ -Ray-Induced Methyl Radicals in Methane Hydrates. *Japanese J. Appl. Phys.* **2004**, *43*, 353–357.

(21) Takeya, K.; Nango, K.; Sugahara, T.; Ohgaki, K.; Tani, A. Activation Energy of Methyl Radical Decay in Methane Hydrate. *J. Phys. Chem. B* **2005**, *109*, 21086–21088.

(22) Tani, A.; Ishikawa, K.; Takeya, K. Thermal Stability of Methyl Radical in γ -Ray Irradiated Methane Hydrate under Different Pressure from 0.003 to 1MPa. *Radiat. Meas.* **2006**, *41*, 1040–1044.

(23) Yeon, S.-H.; Seol, J.; Park, Y.; Koh, D.-Y.; Kang, Y. S.; Lee, H. Spectroscopic Observation of Atomic Hydrogen Radicals Entrapped in Icy Hydrogen Hydrate. *J. Am. Chem. Soc.* **2008**, *130*, 9208–9209.

(24) Muromachi, S.; Ohmura, R.; Takeya, S.; Mori, Y. H. Clathrate Hydrates for Ozone Preservation. *J. Phys. Chem. B* **2010**, *114*, 11430–11435.

